International Journal of Nanomedicine

Dovepress
open access to scientific and medical research

Open Access Full Text Article

ORIGINAL RESEARCH

Stepwise pH-responsive nanoparticles for enhanced cellular uptake and on-demand intracellular release of doxorubicin

This article was published in the following Dove Press journal:
International Journal of Nanomedicine
6 June 2017
Number of times this article has been viewed

Wei-liang Chen[1]
Fang Li[1]
Yan Tang[1]
Shu-di Yang[1]
Ji-zhao Li[1]
Zhi-qiang Yuan[1]
Yang Liu[1]
Xiao-feng Zhou[2]
Chun Liu[3]
Xue-nong Zhang[1]

[1]Department of Pharmaceutics, College of Pharmaceutical Sciences, Soochow University, Suzhou, [2]Department of Ultrasound, Changshu Hospital of Traditional Chinese Medicine, Changshu, [3]Department of Pharmacy, The Hospital of Suzhou People's Hospital Affiliated to Nanjing Medical University, Suzhou, People's Republic of China

Abstract: Physicochemical properties, including particle size, zeta potential, and drug release behavior, affect targeting efficiency, cellular uptake, and antitumor effect of nanocarriers in a formulated drug-delivery system. In this study, a novel stepwise pH-responsive nanodrug delivery system was developed to efficiently deliver and significantly promote the therapeutic effect of doxorubicin (DOX). The system comprised dimethylmaleic acid-chitosan-urocanic acid and elicited stepwise responses to extracellular and intracellular pH. The nanoparticles (NPs), which possessed negative surface charge under physiological conditions and an appropriate nanosize, exhibited advantageous stability during blood circulation and enhanced accumulation in tumor sites via enhanced permeability and retention effect. The tumor cellular uptake of DOX-loaded NPs was significantly promoted by the first-step pH response, wherein surface charge reversion of NPs from negative to positive was triggered by the slightly acidic tumor extracellular environment. After internalization into tumor cells, the second-step pH response in endo/lysosome acidic environment elicited the on-demand intracellular release of DOX from NPs, thereby increasing cytotoxicity against tumor cells. Furthermore, stepwise pH-responsive NPs showed enhanced antiproliferation effect and reduced systemic side effect in vivo. Hence, the stepwise pH-responsive NPs provide a promising strategy for efficient delivery of antitumor agents.

Keywords: stepwise pH-responsive, charge reversal, on-demand drug release, efficient delivery

Introduction

In recent years, nanocarriers have been developed for delivery of chemotherapeutic agents, such as doxorubicin (DOX), to improve antitumor effects and reduce systemic toxicity.[1,2] Nanocarriers for efficient drug delivery should possess the following properties:[3] 1) excellent stability during blood circulation, without significant changes in particle size and undesired drug release, 2) enhanced accumulation in tumor tissues via passive or active targeting effect, 3) improved uptake by tumor cells, and 4) precise and rapid intracellular drug release. However, most nanodrug delivery systems could not efficiently deliver chemotherapy agents because of poor targeting efficiency, low cellular uptake, and slow and incomplete intracellular drug release.[4]

Targeting efficiency and cellular uptake, important indexes of nanoparticles (NPs), are significantly associated with particle size and surface charge of NPs.[5] In general, NPs with particle size of 50–200 nm can passively accumulate in tumor sites via enhanced permeability and retention (EPR) effect.[6] However, as for in vivo applications, the nonspecific reaction between NPs and blood components during circulation may significantly increase the particle size of NPs, leading to reduced passive targeting

Correspondence: Xue-nong Zhang
Department of Pharmaceutics, College of Pharmaceutical Sciences, Soochow University, DuShuHu High Education Zone, Su Zhou 215123, People's Republic of China
Tel +86 512 6588 2087
Fax +86 512 6588 2087
Email zhangxuenong@163.com

submit your manuscript | www.dovepress.com
Dovepress
http://dx.doi.org/10.2147/IJN.S129748

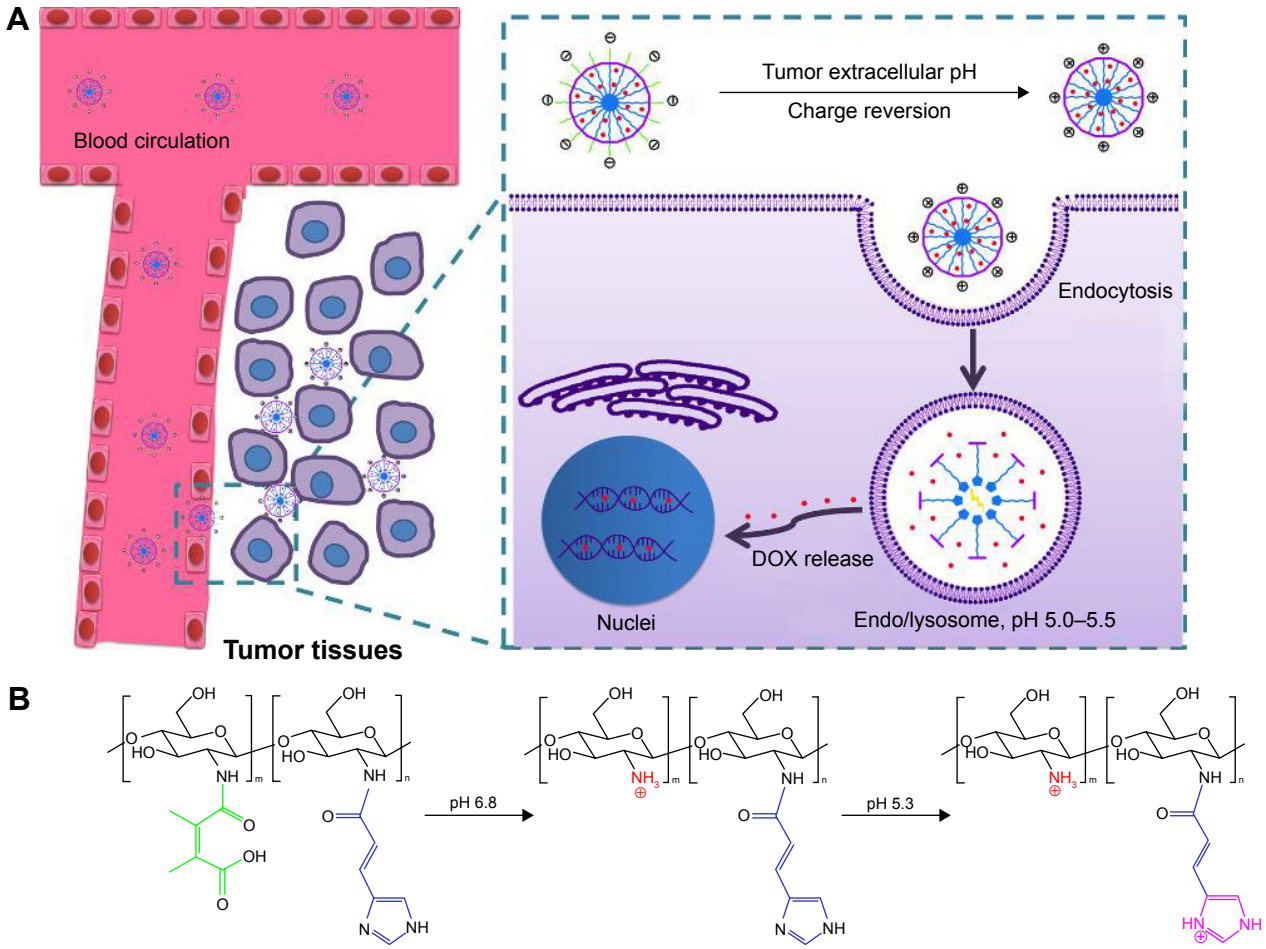

Scheme 1 (**A**) Delivery process of DOX with stepwise pH-responsive NPs. (**B**) pH-responsiveness of the polymer DA-CS-UA.
Abbreviations: DOX, doxorubicin; DA-CS-UA, dimethylmaleic acid-chitosan-urocanic acid; NPs, nanoparticles.

efficiency.[7] Therefore, negatively charged NPs, which are tolerant to adsorption of blood components (such as serum protein), may exhibit excellent serum stability and promote targeting efficiency to tumor. However, negatively charged NPs commonly exhibit low cellular uptake because of their low affinity to the negatively charged tumor cell membranes. In this regard, charge-conversional NPs have gained considerable attention; these particles can reverse surface charge from negative to positive when triggered by extracellular acidic microenvironment (pH 6.5–7.0).[8,9] Yuan et al designed surface charge-switchable NPs based on a zwitterionic polymer modified with 2,3-dimethylmaleic anhydride (DMMA).[10] These NPs, which are negatively charged during circulation, were inert to serum component adsorption to ensure the targeting efficiency in tumor sites. Moreover, these NPs could switch surface charge to positive and enhance cellular uptake by shedding negatively charged DMMA part in response to the slightly acidic extracellular conditions. Previous studies showed that charged-conversional NPs gained satisfactory balance between targeting efficiency and cellular uptake.[11–13]

Slow and incomplete drug release within tumor cells is another challenge for efficient delivery of antitumor agents since most antitumor drugs achieve their therapeutic effects by reacting with nuclei or organelles.[14] As such, stimuli-responsive NPs, based on the specific microenvironment of tumor regions, have been increasingly designed for delivery of antitumor agents.[15] Intracellular biological signals, such as acidic pH, high concentration of glutathione, and enzymes, can be adopted for stimuli-triggered precise intracellular drug release to enhance the therapeutic effects and reduce systemic toxicity.[16] Among these smart NPs, pH-responsive NPs responding to the endo/lysosomal pH have been comprehensively studied considering that endo/lysosome have significantly lower pH (pH 5.0–5.5) than physiological conditions (pH 7.35–7.45).[17,18] Imidazole group in urocanic acid (UA)-grafted polymers, with pKa of 6.0, would be pronated in response to endo/lysosome pH and caused the breakdown of the hydrophilic/hydrophobic balance of formulated NPs.[19] NPs based on these polymers show a rapid, precise drug release within tumor cells and enhanced antitumor effects.

To date, few studies have reported NPs that could simultaneously respond to both extracellular pH and endo/lysosomal pH to enhance cellular uptake and achieve precise intracellular drug release. In this study, novel stepwise pH-responsive NPs were designed by self-assembling polymer dimethylmaleic acid-chitosan-UA (DA-CS-UA) that are used to deliver DOX, a frequently used antitumor agent. The polymer was synthesized based on CS, with UA as hydrophobic segment; the polymer was then modified with DMMA to protect the positive charge.[20,21] DOX-loaded DA-CS-UA NPs (DOX/DA) exhibited negative charge under physiological conditions to reduce nonspecific protein absorption and improve the targeting efficiency to tumor. Once passively arriving at tumor tissues via EPR effect, the first-step pH response was triggered by the extracellular pH, which switched the surface charge of NPs from negative to positive through the cleavage of DMMA shielding, resulting in enhanced cellular uptake. Afterward, the second-step pH response was triggered in endo/lysosome acidic environment and payloads were released within cells rapidly and completely, which caused the apoptosis of tumor cells. The preparation, physicochemical properties, cellular uptake, cytotoxicity, targeting efficiency, and antitumor effects of stepwise pH-responsive NPs were studied. The positively charged unmodified CS-UA NPs (UA-NPs) within the pH range from 7.4 to 6.8 and the negatively charged (succinyl-CS-UA) SA-CS-UA NPs (SA-NPs) without charge reversion property responding to the extracellular pH were used for comparison.

Materials and methods

Materials

CS with molecular weight (MW) of 3–5 kDa and deacetylation degree of 90% was obtained from Qingdao Yunzhou Biochemistry Co., Ltd (Qingdao, People's Republic of China). 3-(3-dimethylaminopropyl)-1-ethylcarbodiimide hydrochloride (EDC·HCl), N-hydroxysuccinimide (NHS), and UA were purchased from Adamas-beta-Reagent Co., Ltd (Shanghai, People's Republic of China). DMMA was from Sinopharm Chemical Reagent Co., Ltd (Shanghai, People's Republic of China). Doxorubicin hydrochloride (DOX·HCl) of over 98% purity was obtained from Melone Pharmaceutical Co., Ltd (Dalian, People's Republic of China). Methyl thiazolyl tetrazolium bromide (MTT) was from Sigma-Aldrich (St Louis, MO, USA). Hoechst 33258 and LysoTraker Green were from Invitrogen (Eugene, OR, USA). Roswell Park Memorial Institute (RPMI)-1640 was purchased from Hyclone Thermo-Fisher Biochemical Products Co., Ltd (Beijing, People's Republic of China). Fetal bovine serum (FBS) was obtained from Zhejiang Tianhang Biotechnology Co., Ltd (Hangzhou, People's Republic of China). Trypsin ethylenediaminetetraacetic acid solution and penicillin-streptomycin solution were from Beyotime Institution of Biotechnology (Shanghai, People's Republic of China). All other chemicals were of analytical grade and used without further purification.

Murine breast cancer cell lines 4T1 from Jiangsu Province Key Laboratory of Biotechnology and Immunology (Suzhou, People's Republic of China) were cultured in RPMI-1640 with 10% (v/v) FBS and 1% (v/v) penicillin-streptomycin solution under 37°C and 5% CO_2 condition.

Female nude mice (BALB/C, nu/nu) (16±2 g) were purchased from the Shanghai SLAC Laboratory Animals Co. Ltd (Shanghai, People's Republic of China) and raised in specific pathogen free condition. All animal protocols were approved by the Institutional Animal Care and Use Committee of Soochow University and were in compliance with the Guidelines for the Care and Use of Laboratory Animals (Chinese-National-Research-Council, 2006) and "ARRIVE" guidelines.

Synthesis and characterization of DA-CS-UA

Synthesis of CS-UA

CS-UA was synthesized by reacting amine groups of CS and carboxyl group of UA.[22] Briefly, UA (138 mg) was dissolved in 10 mL of *N*,*N*-dimethylformamide. Subsequently, EDC·HCl (400 mg) and NHS (230 mg) were added to activate the carboxyl group of UA. The solution mixture was added into the CS solution (240 mg dissolved in 30 mL of phosphate buffer solution [PBS, pH 7.4]) while stirring. The reaction was performed at 50°C for 24 h. The product was dialyzed against distilled water for 2 days and then lyophilized.

Synthesis of DA-CS-UA and SA-CS-UA

Polymer DA-CS-UA was obtained by reacting CS-UA with DMMA.[23] CS-UA (100 mg) was dissolved in 30 mL of PBS (0.1 M, pH 8.5), and two equivalents of DMMA (157 mg) were slowly added; the pH of the solution was maintained at 8.0–8.5 by simultaneous addition of 0.2 M NaOH solution. The reaction was performed at room temperature for 6 h, and DA-CS-UA was obtained by lyophilization. The synthesis of SA-CS-UA was similar to that of DA-CS-UA, except that SA, instead of DMMA, was added to react with SA-CS-UA.

Characterization of CS-UA, DA-CS-UA, or SU-CS-UA

CS, CS-UA, DA-CS-NA, and SA-CS-NA were dissolved in distilled water, and their hydrogen-1 nuclear magnetic resonance (^{1}H NMR) spectra were obtained using a Bruker

(AVACE) AV-500 spectrometer. The degree of substitution, which was defined as the number of UA, DMMA, or SA molecules per 100 sugar residues of CS, was studied using ^{1}H NMR.

Preparation and characterization of stepwise pH-responsive NPs

Preparation of blank NPs

The blank NPs (1 mg/mL) formed from CS-UA, DA-CS-UA, or SA-CS-UA (abbreviated as UA-NPs, DA-NPs, or SA-NPs, respectively) were prepared by sonication method. Briefly, 10 mg of polymers (CS-UA, DA-CS-UA, or SA-CS-UA) was dissolved in 10 mL of distilled water, sonicated (200 W) for 100 times with a probe ultrasound machine, and filtered three times with a 0.22 μm membrane.

pH-triggered particle size and zeta potential charge

Blank NPs (1 mg/mL, 1 mL) were incubated with PBS (4 mL) of different pH levels (pH 7.4, 6.8, or 5.3) at 37°C for 2 h. Subsequently, the particle size and zeta potential were measured with dynamic light scattering (DLS) method (Malvern Nano-ZS90; Zetasizer, Malvern, UK).

Adsorption of proteins on NPs

The adsorption of proteins on NPs was carried out by incubating UA-NPs, DA-NPs, or SA-NPs (1 mg/mL, 1 mL) with bovine serum albumin (1 mL) at 37°C and at pH 7.4 or pH 6.8 for 2 h.[10] The mixture was centrifuged (12,000 rpm) for 30 min to separate NPs and free proteins. Afterward, the protein concentration was measured by Bradford method and protein adsorption was determined.

Serum stability study

About 1 mL of UA-NPs, DA-NPs, or SA-NPs (1 mg/mL) was incubated with the same volume of FBS at 37°C.[24] At designed time points, 0.2 mL of mixture was taken out and the absorbance was measured at a wavelength of 630 nm with a microplate reader. The relative turbidity was calculated with the absorbance at t=0 h of each group set as 100%.

Preparation and characterization of DOX-loaded NPs

DOX-loaded UA-NPs, DA-NPs, and SA-NPs (abbreviated as DOX/UA, DOX/DA, and DOX/SA, respectively) were prepared by dialysis method.[25] DOX·HCl (5 mg) was dissolved in DMSO (1 mL) and desalted with triethylamine (50 μL). DOX solution in DMSO was then added to blank NP solutions (10 mL, 1 mg/mL), dialyzed against PBS (0.1 M, pH 7.4) for five times, and filtered three times through 0.22 μm membranes to obtain the final DOX-loaded NPs. The particle size and zeta potential of NPs were detected by DLS (Zetasizer). The encapsulation efficiency (EE%) and drug-loading content (DLC%) of DOX in different formulations were determined and the concentration of DOX was measured using a fluorescence spectrophotometer at an excitation wavelength of 480 nm and emission wavelength of 590 nm. An ultrafiltration method was used to separate free DOX and DOX-loaded NPs. The EE% and DLC% of DOX-loaded NPs were calculated by the following equations:[26]

$$\mathrm{EE\%} = \frac{w_0}{w_1} \times 100\% \quad (1)$$

$$\mathrm{DLC\%} = \frac{w_0}{w} \times 100\% \quad (2)$$

where w_0 and w_1 are the amount of loaded DOX and total weight of DOX in solution, respectively, and w is the total weight of DOX-loaded NPs.

Drug release from DOX-loaded NPs in vitro

Drug release from DOX-loaded NPs was studied at 37°C under different PBS conditions (pH 7.4, 6.8, or 5.3) by dialysis bag method.[27] DOX-loaded NPs (5 mL) were added to a dialysis bag (MWCO 3,500 Da), which was placed in a container with PBS (100 mL) of different pH levels as corresponding mediums. At designed time points, 1 mL of the corresponding medium from each group was collected for concentration determination and replaced with an equal volume of fresh medium.

Cellular uptake and intracellular distribution

Cellular uptake and intracellular distribution of DOX in different formulations were studied using a confocal laser scanning microscopy (CLSM).[28] 4T1 cells cultured in six-well plates were incubated with DOX·HCl or DOX-loaded NPs (final concentration of DOX was 5 μg/mL) under pH 7.4 or 6.8 for 2 h. Afterward, the nuclei were stained with Hoechst 33258. The cells were fixed with paraformaldehyde and observed by CLSM.

Flow cytometry was used to study the quantitative uptake of DOX in different formulations by 4T1 cells after the incubation with DOX·HCl or DOX-loaded NPs (final concentration of DOX was 5 μg/mL) at pH 6.8 or 7.4 for 2 h.

For intracellular tracking study, NPs were labeled with fluorescein isothiocyanate isomer I (FITC) and incubated with 4T1 cells at pH 7.4 for 2 h.[29] The cells were fixed and observed by CLSM. To evaluate the co-location of DOX with nuclei, DOX-loaded NPs were incubated with 4T1 cells for 6 h and observed by CLSM.

Cytotoxicity study

The cytotoxicity of polymers and DOX in different formulations was studied by MTT assay.[23] 4T1 cells were seeded in 96-well plates (2,000 cells/well) and cultured for 24 h. The polymers or DOX formulations in different concentrations were subsequently added at pH 7.4 or 6.8 and incubated for 6 h. Later, the medium was replaced with a fresh one and incubated for another 18 h. The cell viability of each group was determined by MTT assay.

The cytotoxicity of different formulations against 4T1 cells was calculated using the following equation:

$$\text{Cell viability (\%)} = \frac{A_{570(\text{treated})} - A_0}{A_{570(\text{non-treated})} - A_0} \times 100\% \quad (3)$$

where $A_{570(\text{treated})}$ represents the absorbance of cells treated with polymers or DOX formulations at 570 nm, $A_{570(\text{non-treated})}$ represents the absorbance of cells in non-treated group, and A_0 represents the non-cell group.

Tumor penetrability evaluation

The tumor penetrability of DOX-loaded NPs was studied by observing DOX distribution in three-dimensional (3D) tumor spheroids under different pH values. 3D tumor spheroids were prepared by seeding 4T1 cells in 96-well plates coated with 80 μL of 2% low melting-temperature agarose and incubating for several days. Then the tumor spheroids were incubated with DOX-loaded NPs for 2 h, followed by washing with PBS for three times and observed under CLSM.

Targeting effect in vivo

In vivo near-infrared (NIR) fluorescence imaging

4T1 tumor-bearing mice models were constructed by subcutaneous injection of 4T1 cells (2×10^6 cells for each mouse). 1,1′-dioctadecyl-3,3,3′,3′-tetramethylindotricarbocyanine iodide (DiR) was used as a fluorescent probe to study the targeting effect of NPs on tumor-bearing mice with an in vivo NIR fluorescence imaging system (IVIS Lumina II).[30] DiR-loaded NPs (DiR/UA, DiR/DA, and DiR/SA) were prepared by solvent evaporation method at a final DiR concentration of 50 μg/mL. Afterward, DiR-loaded NPs were injected intravenously into tumor-bearing mice (5 μg DiR for each mouse), and the mice were observed at 2, 6, 12, 24, and 48 h post-injection. Later, the mice were sacrificed, and the main organs, including heart, liver, spleen, lung, kidney, and tumor, were excised for NIR fluorescence imaging.

Biodistribution of DOX in tumor-bearing mice

4T1 tumor-bearing mice were given different formulations of DOX via tail vein at a dose of 5 mg/kg. After 24 h, tumor and main organs, including heart, liver, spleen, lung, and kidney, were excised and homogenized after sacrificing the mice. DOX in tumor and main organs was extracted using mixed organic solvents (chloroform/methanol =3/1).[31] The DOX concentration was measured using a multifunctional microplate reader, and the ratio of DOX amount to organ weight was calculated.

Antitumor efficiency in vivo

4T1 tumor-bearing mice were prepared as mentioned earlier and divided into five groups with four mice in each group. Various formulations, including saline, DOX·HCl, and DOX-loaded NPs, were intravenously injected into the mice at DOX dose of 5 mg/kg every 4 days (days 1, 5, and 9) since the tumors reached a volume of 50–80 mm^3. The tumor volumes and body weight of mice were detected every 2 days. The mice were sacrificed on day 15, and the tumors were excised for weighing and imaging.

Statistical analysis

All the experiments were conducted for at least three times. All data were presented as mean ± standard deviation (SD). Results were analyzed by ANOVA and Student's *t*-test was used for pair-wise comparisons. Statistical significance was showed as $^{***}P<0.001$, $^{**}P<0.01$, and $^{*}P<0.5$.

Results and discussions

Synthesis and characterization

As shown in Figure 1A, firstly, CS-UA was synthesized by the amide reaction between the amine groups of CS and carboxyl groups of UA. Afterward, CS-UA was modified with DMMA to obtain DA-CS-UA. As a comparison, SA-CS-UA was also synthesized by the same method, except that SA, instead of DMMA, was used. The structure of DA-CS-UA and SA-CS-UA characterized using ^{1}H NMR spectra is shown in Figure 1B and Figure S1. δ 3.2–4.0, 7.2, 1.6–1.8, and 2.2–2.5 ppm refer to the hydrogen atom in CS, imidazole, DA, and SA groups, respectively. The DS of UA, DA, and SA calculated from ^{1}H NMR spectra was 12.9%, 15.3%, and 19.5%, respectively.

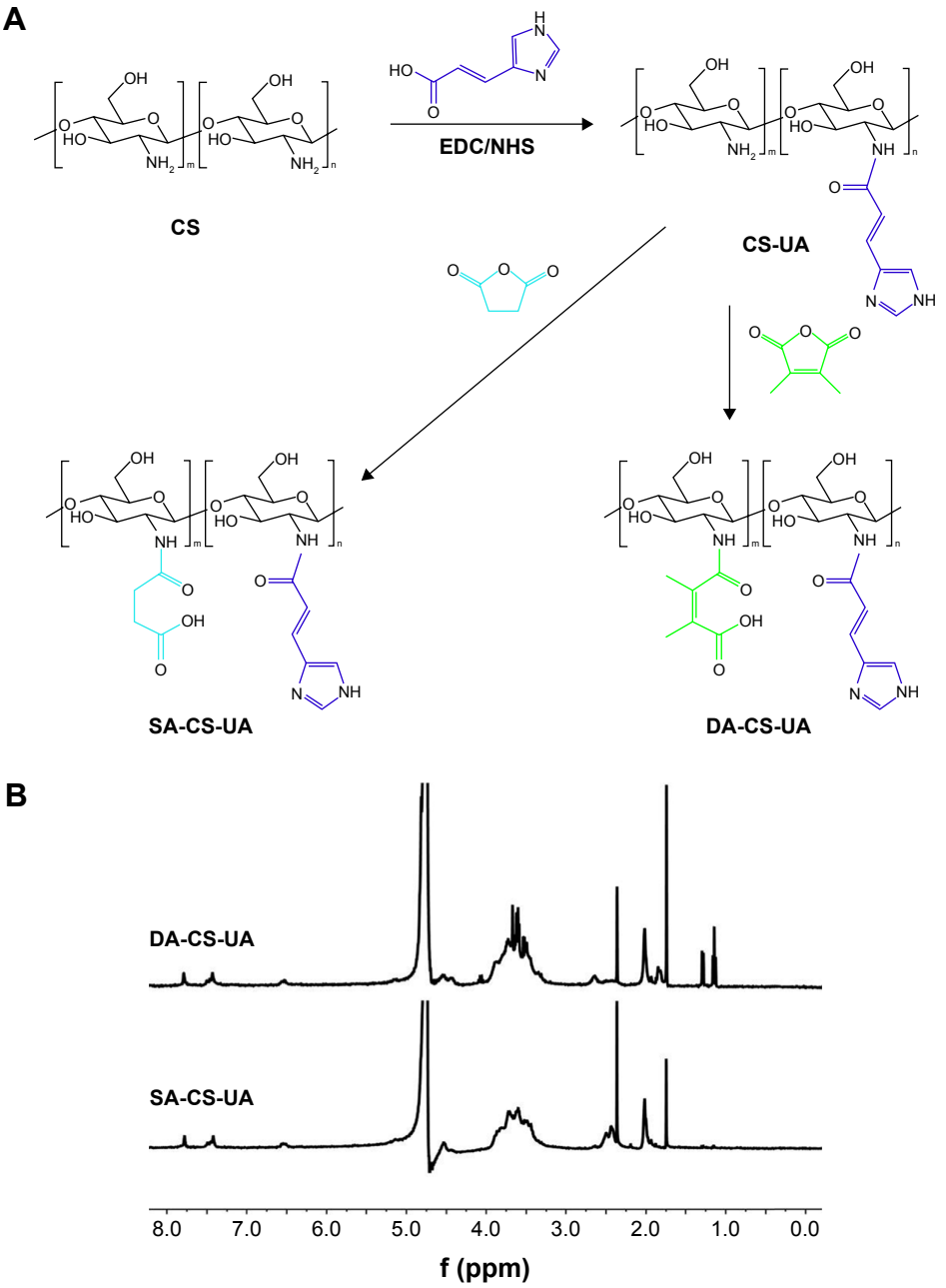

Figure 1 Synthesis (**A**) and ^{1}H NMR spectra (**B**) of DA-CS-UA and SA-CS-UA polymers.
Abbreviations: DA-CS-UA, dimethylmaleic acid-chitosan-urocanic acid; EDC, 3-(3-dimethylaminopropyl)-1-ethylcarbodiimide; ^{1}HNMR, hydrogen-1 nuclear magnetic resonance; NHS, N-hydroxysuccinimide; ppm, parts per million; SA-CS-UA, succinyl-chitosan-urocanic acid.

Preparation and characterization of stepwise pH-responsive NPs

The blank NPs assembled from three polymers were prepared, and the pH-responsive behavior of DA-NPs was studied by measuring the particle size and zeta potential, with DA-NPs and SA-NPs used as comparisons. As shown in Figure 2A, UA-NPs, DA-NPs, and SA-NPs were prepared with particle size of 100–160 nm, and the particle sizes of DA-NPs and SA-NPs were relatively larger than that of UA-NPs. After 2 h of incubation at pH 6.8, DA-NPs showed a slight increase in particle size from 157.9 nm to 189.3 nm. A lower pH (pH 5.3) showed a significant influence in particle size of DA-NPs; the particle size increased to more than 1,000 nm, and the particle size distribution showed double peaks. As shown in Figure 2B, UA-NPs exhibited a positive charge at pH 7.4, whereas DA-NPs and SA-NPs showed a negative charged because of the modification of carboxyl groups. DA-NPs showed a charge reversion property in response to the acidic pH (pH 6.8), which perhaps resulted from the shedding of negatively charged DMMA groups.[32]

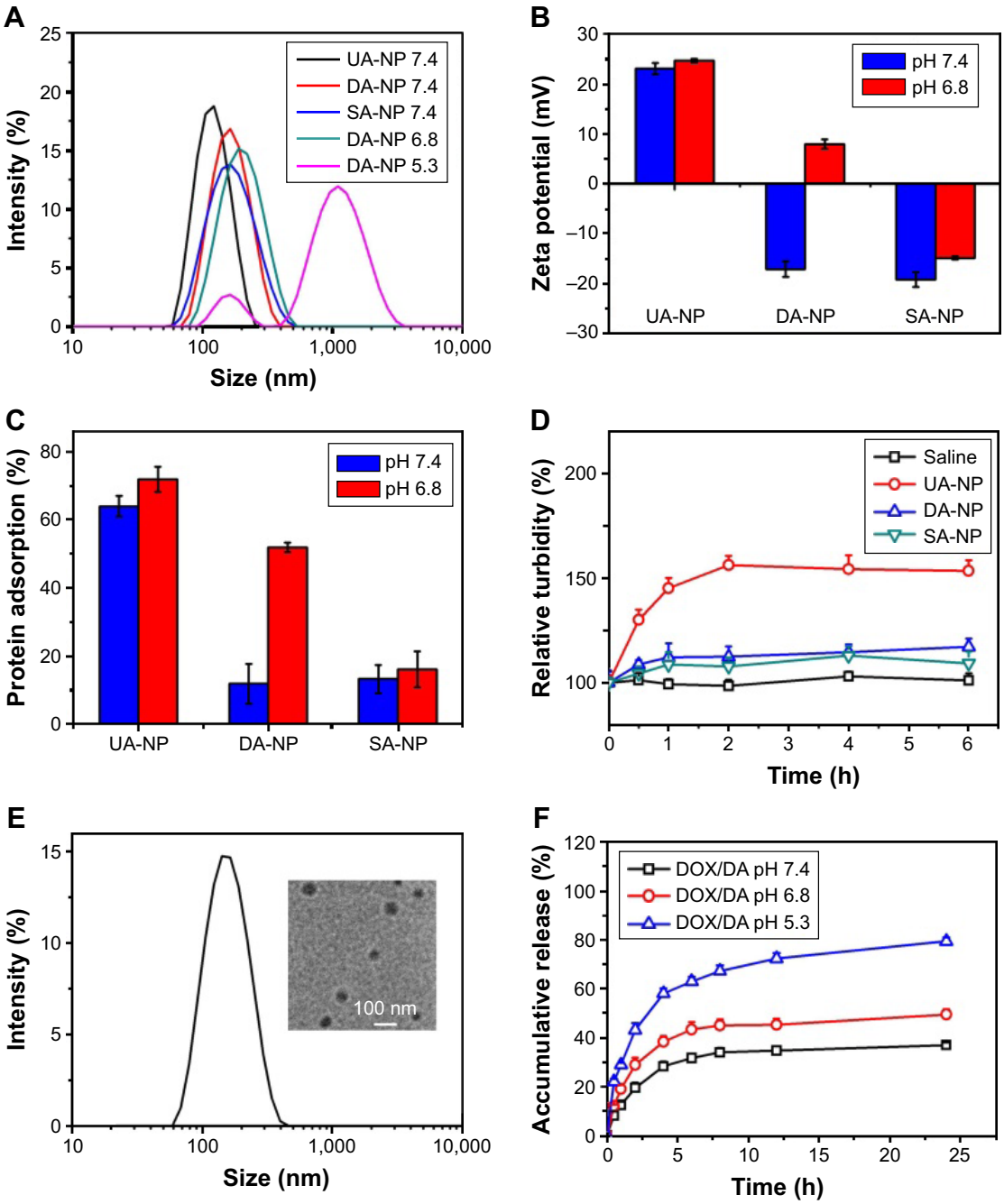

Figure 2 Characterization of DOX-loaded NPs. Particle size (**A**), zeta potential (**B**), protein adsorption (**C**), and serum stability (**D**) of blank NPs at different pH values. Particle size distribution and TEM of DOX/DA (**E**), and DOX release from DOX/DA in vitro (**F**).
Abbreviations: DA, dimethylmaleic acid; DOX, doxorubicin; NPs, nanoparticles; SA, succinic anhydride; TEM, transmission electron microscope; UA, urocanic acid.

However, the low pH environment almost showed no influence on the zeta potential of both UA-NPs and SA-NPs. As shown in Figure 2C, at pH 7.4, the negatively charged DA-NPs and SA-NPs exhibited considerably lower protein adsorption than the positively charged UA-NPs. Nevertheless, at pH 6.5, the zeta potential of DA-NPs changed from negative to positive, thereby leading to a remarkable adsorption of protein. In addition, at physiological condition, the negatively charged DA-NPs and SA-NPs elicited no significant aggregation during the incubation with FBS (Figure 2D), which suggested that they possessed an excellent serum stability. The results indicated that DA-NPs, with a negative zeta potential, would avoid nonspecific adsorption with negatively charged serum protein and exhibit a favorable stability during blood circulation, which was beneficial to the passive target efficacy to solid tumors in vivo via the EPR effect.[33]

Moreover, the charge reversion property of DA-NPs in response to the extracellular acidic condition could play an important role in the internalization into tumor cells.

Preparation of DOX-loaded NPs and DOX release in vitro

DOX-loaded NPs were prepared by dialysis method, and the particle size, zeta potential, EE%, DLC%, and release behaviors were studied. As shown in Table 1, the DOX-loaded NPs exhibited a suitable particle size and relatively high EE% and DLC%. DOX-loaded NPs showed no significant difference from the blank NPs in particle size or zeta potential. DOX/UA, DOX/DA, and DOX/SA exhibited similar DOX release behavior to each other (Figure 2F and Figure S2), with less than 40% of DOX released within 24 h at pH 7.4; this observation suggested that they exhibited a delayed release property during the blood circulation. Extracellular pH (pH 6.8) showed no significant influence on the DOX release from DOX-loaded NPs, with a bit more DOX released compared with that at pH 7.4. However, a rapid DOX release behavior was observed at pH 5.3, which might be due to the hydrophilization of the hydrophobic core in response to the acidic pH (pH <6.0).[34] The result indicated that DOX would release rapidly from NPs within the acidic endo/lysosome, which could increase the antitumor effect of DOX.

Uptake study and cytotoxicity of DOX-loaded NPs

The cellular uptake of DOX-loaded NPs was studied using CLSM and flow cytometry at different pH values to identify the effect of charge reversion property. As shown in Figure 3A, when incubated for 2 h at pH 7.4, the positively charged DOX/UA exhibited a higher cellular uptake than that of the negatively charged DOX/DA and DOX/SA, which might be contributed to the higher affinity between the positively charged NPs and negatively charged cell membranes. When the incubation pH decreased to 6.8, the pH-triggered charge reversion elicited apparently enhanced cellular uptake (Figure 3B).[35] Nonetheless, the decreased pH exhibited no significant influence on the uptake of DOX·HCl, DOX/UA, or DOX/SA. The quantitative uptake results of DOX using flow cytometry are shown in Figure 3C and Figure S3, which were in accordance with the uptake study observed by CLSM. At both pH 7.4 and 6.8, DOX-loaded NPs showed a significantly higher cellular uptake than DOX·HCl. Notably, the pH decrease from 7.4 to 6.8 displayed significant influence on the cellular uptake of DOX/DA group, where a 1.56-fold stronger fluorescence intensity at pH 6.8 was observed (Figure 3C). No obvious changes occurred in both DOX/SA and DOX/UA groups. These results indicated that DOX/DA with negative charge and relatively low cellular uptake during the circulation (pH 7.4) could gain an excellent cellular uptake at the acidic tumor sites (pH 6.8) as a result of the charge reversion property.

Table 1 Characterization of DOX-loaded NPs

Formulation	Particle size (nm)	Zeta potential (mV)	EE (%)	DLC (%)
DOX/UA	122.5±3.2	23.0±1.1	92.8±3.7	26.3±3.3
DOX/DA	141.3±3.2	−19.2±1.5	89.4±2.6	24.6±2.8
DOX/SA	145.2±2.7	−17.1±1.6	88.3±4.1	25.1±1.9

Abbreviations: DA, dimethylmaleic acid; DLC, drug-loading content; DOX, doxorubicin; EE, encapsulation efficiency; NPs, nanoparticles; UA, urocanic acid; SA, succinic anhydride; DOX/UA, DOX-loaded CS-UA NPs; DOX/DA, DOX-loaded DA-CS-UA NPs; DOX/SA, DOX-loaded SA-CS-UA NPs.

The intracellular tracking and distribution of NPs were studied using CLSM. As shown in Figure 4A, after incubation for 2 h, FITC-labeled NPs mainly located in cytoplasm and co-located with endo/lysosome facilitated the pH-triggered DOX release.[36] Afterward, the free DOX released from NPs diffused to the whole cell and showed co-location with nuclei, which was beneficial to the antitumor effect of DOX (Figure 4B).

The cytotoxicity against 4T1 cells of blank NPs and DOX in different formulations was studied by MTT assay. As shown in Figure S4, the blank NPs, including UA-NPs, DA-NPs and SA-NPs, exhibited almost no cytotoxicity against 4T1 cells. As shown in Figure 4C and D, DOX formulations exhibited a concentration-dependent cytotoxicity against 4T1 cells at pH 7.4 or 6.8. At pH 7.4, among the DOX-loaded NPs, DOX/UA exhibited the highest cytotoxicity against 4T1 cells, with a significantly lower half maximal inhibitory concentration (IC_{50}) than DOX/DA and DOX/SA ($P<0.01$), which might have resulted from the highest uptake amount. Notably, the decrease in incubation pH value significantly enhanced the cell killing ability of DOX/DA, and no obvious differences were observed in other DOX formulations. Therefore, the charge reversion property of DOX/DA might have enhanced the internalization of DOX/DA and improved the cytotoxicity against 4T1 cells. Although the cellular uptake of DOX·HCl was not as high as that of DOX-loaded NPs, DOX·HCl exhibited a higher cytotoxicity, which might be due to the rapid co-location of DOX·HCl and nuclei.[37]

Tumor penetrability evaluation

3D tumor spheroids were used to investigate the tumor penetrability of DOX-loaded NPs. As shown in Figure 5 and Figure S5, at pH 7.4, the positively charged DOX/UA

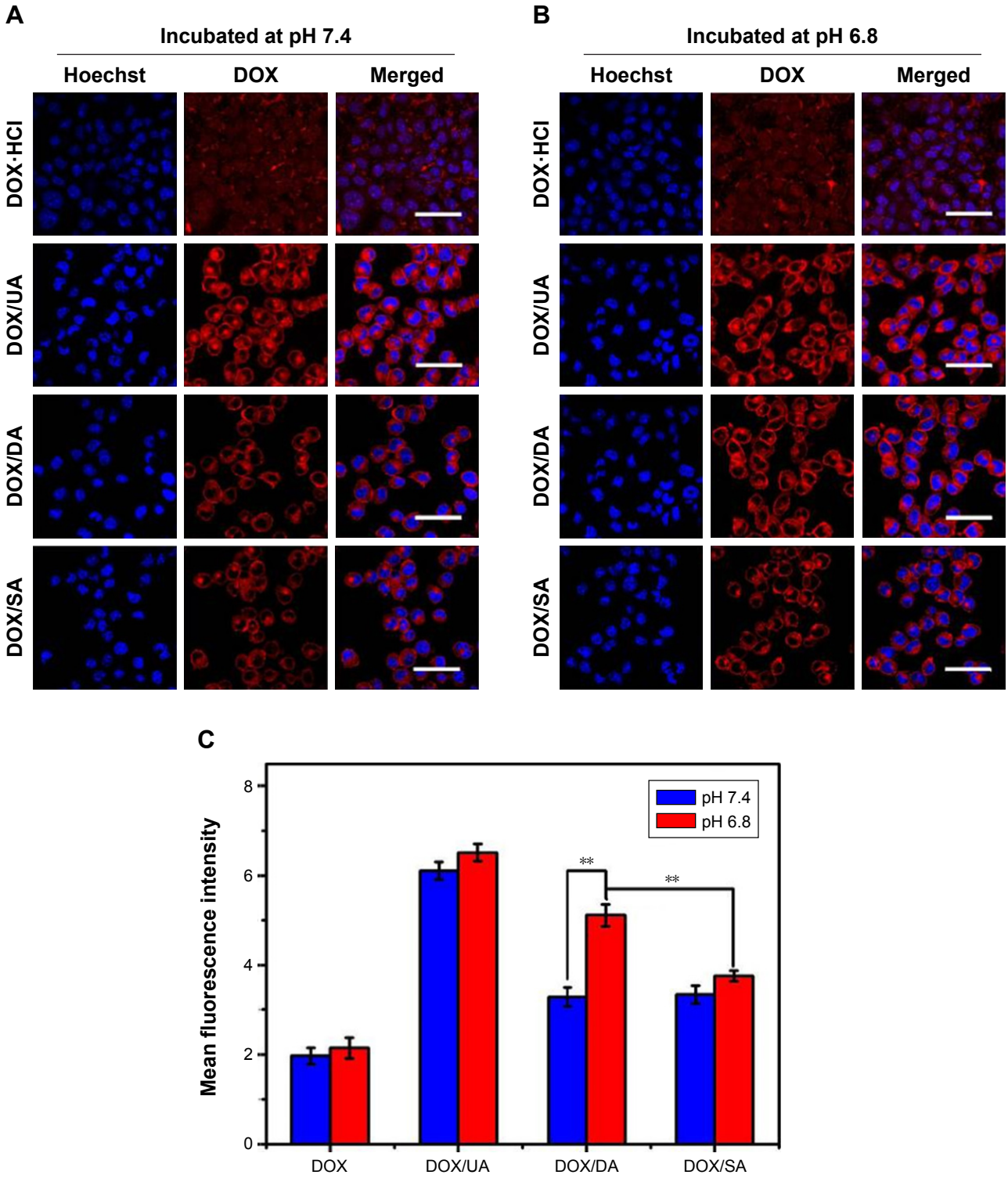

Figure 3 Uptake of DOX in different formulations. Uptake of DOX when incubated for 2 h at pH 7.4 (**A**) or 6.8 (**B**), as observed by CLSM (bar 50 μm). Mean fluorescence intensity of 4T1 cells treated with DOX-loaded NPs, studied with flow cytometry (**C**). DOX concentration was 5 μg/mL.
Note: Statistical significance is shown as $^{**}P<0.01$.
Abbreviations: DA, dimethylmaleic acid; DOX, doxorubicin; DOX·HCl, doxorubicin hydrochloride; NPs, nanoparticles; SA, succinic anhydride; UA, urocanic acid.

exhibited better tumor penetrability than the negatively charged DOX/DA and DOX/SA. As pH decreased, the tumor penetrability of DOX/DA was improved, while that of DOX/SA was still unsatisfied. It suggested that under the tumor acidic microenvironment the charge reversal DOX/DA could reverse the surface charge from negative to positive, which is benefited for the tumor penetrability (Figure S5). With better tumor penetrability, DOX/DAs were easier to get

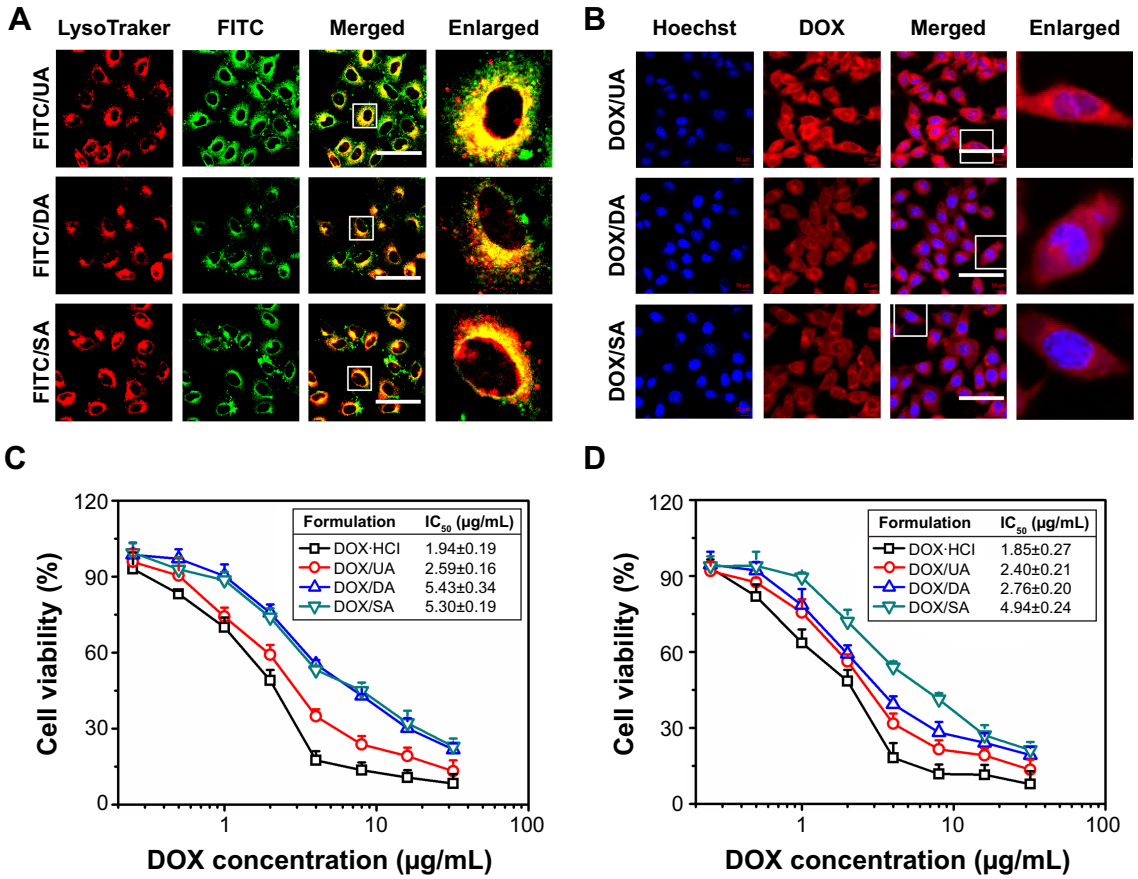

Figure 4 Co-location of NPs with endo/lysosome (**A**) and nuclei (**B**) (bar 50 μm). Cytotoxicity of DOX in different formulations at pH 7.4 (**C**) or 6.8 (**D**).
Abbreviations: DA, dimethylmaleic acid; DOX, doxorubicin; DOX·HCl, doxorubicin hydrochloride; FITC, fluorescein isothiocyanate isomer I; IC_{50}, half maximal inhibitory concentration; NPs, nanoparticles; SA, succinic anhydride; UA, urocanic acid.

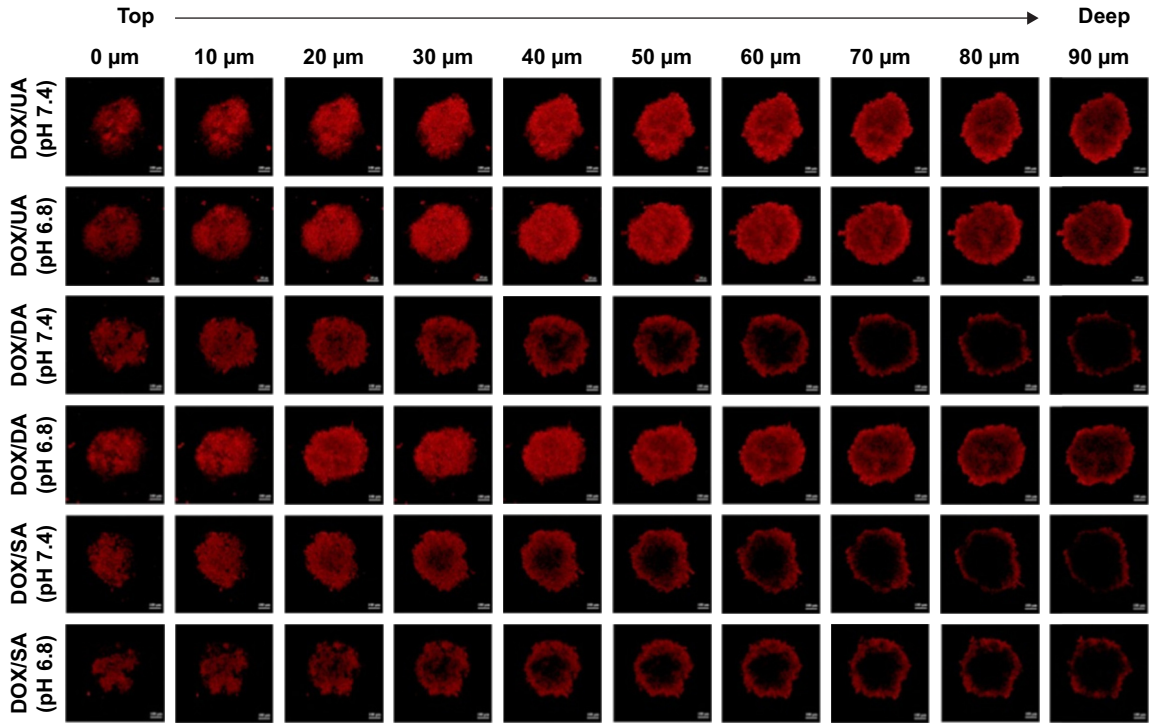

Figure 5 Distribution of DOX-loaded NPs in 3D tumor spheroids under different pH values.
Note: Scale bar: 100 μm.
Abbreviations: 3D, three dimensional; DA, dimethylmaleic acid; DOX, doxorubicin; DOX·HCl, doxorubicin hydrochloride; NPs, nanoparticles; SA, succinic anhydride; UA, urocanic acid.

into the deep area of tumor tissues and obtain an enhanced antitumor efficiency.[38]

Targeting effect to tumor in vivo

DiR, a near-infrared fluorescent probe, was encapsulated into NPs to study the targeting effect of NPs in vivo. As shown in Figure 6A, negatively charged DiR/DA and DiR/SA with better serum stability showed a better targeting effect toward solid tumors via the EPR effect, compared with positively charged DiR/UA. DiR/DA, which could reverse the surface charge from negative to positive and enhance the cellular uptake, showed higher fluorescence intensity in tumor tissues than DiR/SA (Figure 6A and B). The biodistribution of DOX formulations was also studied to evaluate the targeting effect in vivo quantitatively. As shown in Figure 7C, similar to the aforementioned NIR imaging results, the accumulation amount of DOX/DA in tumor tissue was considerably higher than that of DOX/UA and DOX/SA ($P<0.01$), thereby indicating that DOX/DA possessed satisfied targeting efficiency to tumor in vivo. Furthermore, DiR- or DOX-loaded NPs exhibited significant accumulation in liver and spleen, which might be due to the capture of reticular endothelial system.[39] Additionally, DOX·HCl exhibited significant accumulation in heart but relatively low accumulation in tumor, which suggested that the injection of DOX·HCl might lead to unavoidable cardiotoxicity and unsatisfied antitumor effect.

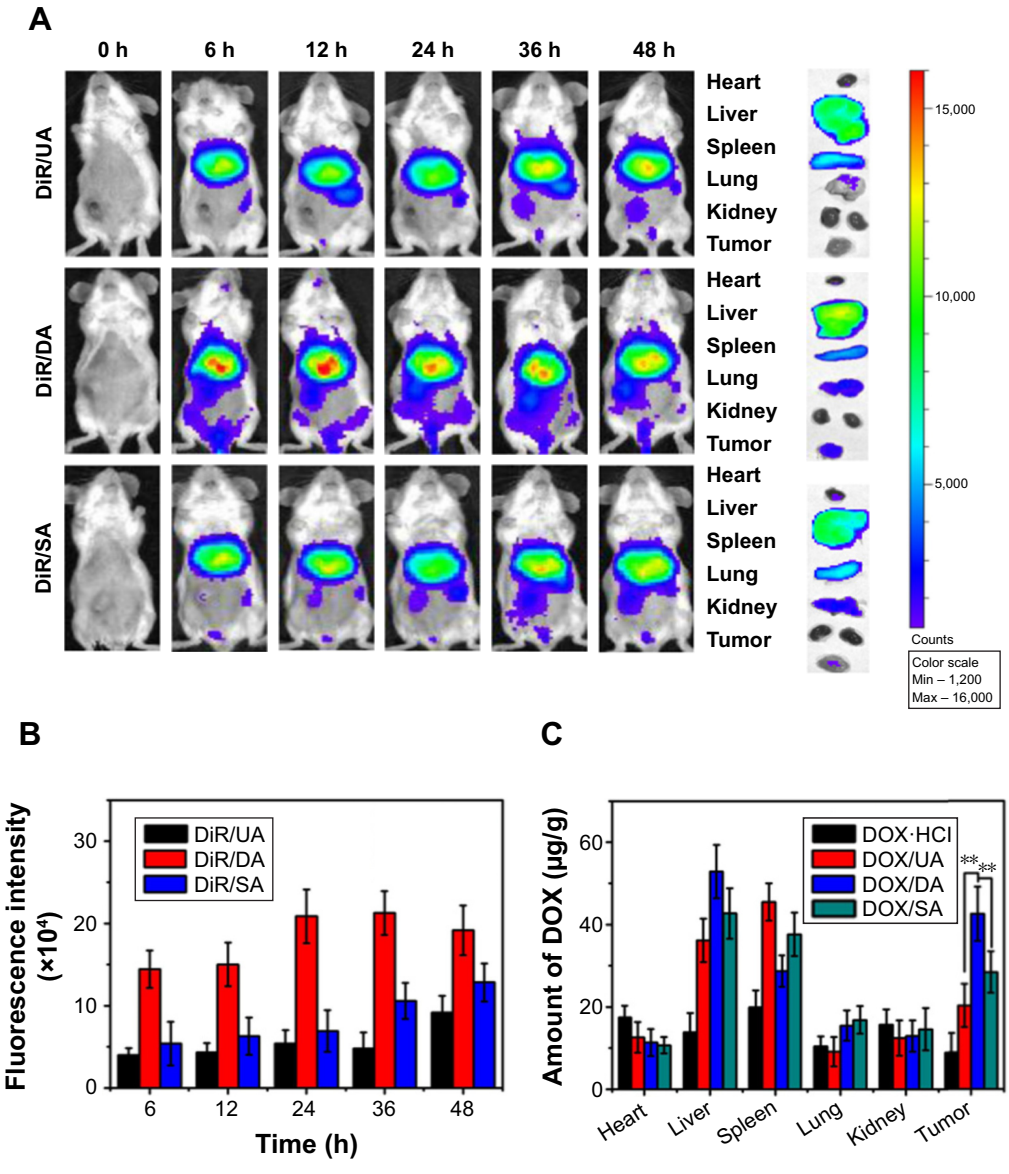

Figure 6 Targeting efficiency in vivo. Imaging of tumor-bearing mice injected with DiR-loaded NPs (**A**). Fluorescence intensity of DiR in tumor area (**B**). Biodistribution of DOX in tumor-bearing mice (**C**).

Note: Statistical significance is shown as $^{**}P<0.01$.

Abbreviations: DA, dimethylmaleic acid; DiR, 1,1′-dioctadecyl-3,3,3′,3′-tetramethylindotricarbocyanine; DOX, doxorubicin; DOX·HCl, doxorubicin hydrochloride; NPs, nanoparticles; SA, succinic anhydride; UA, urocanic acid.

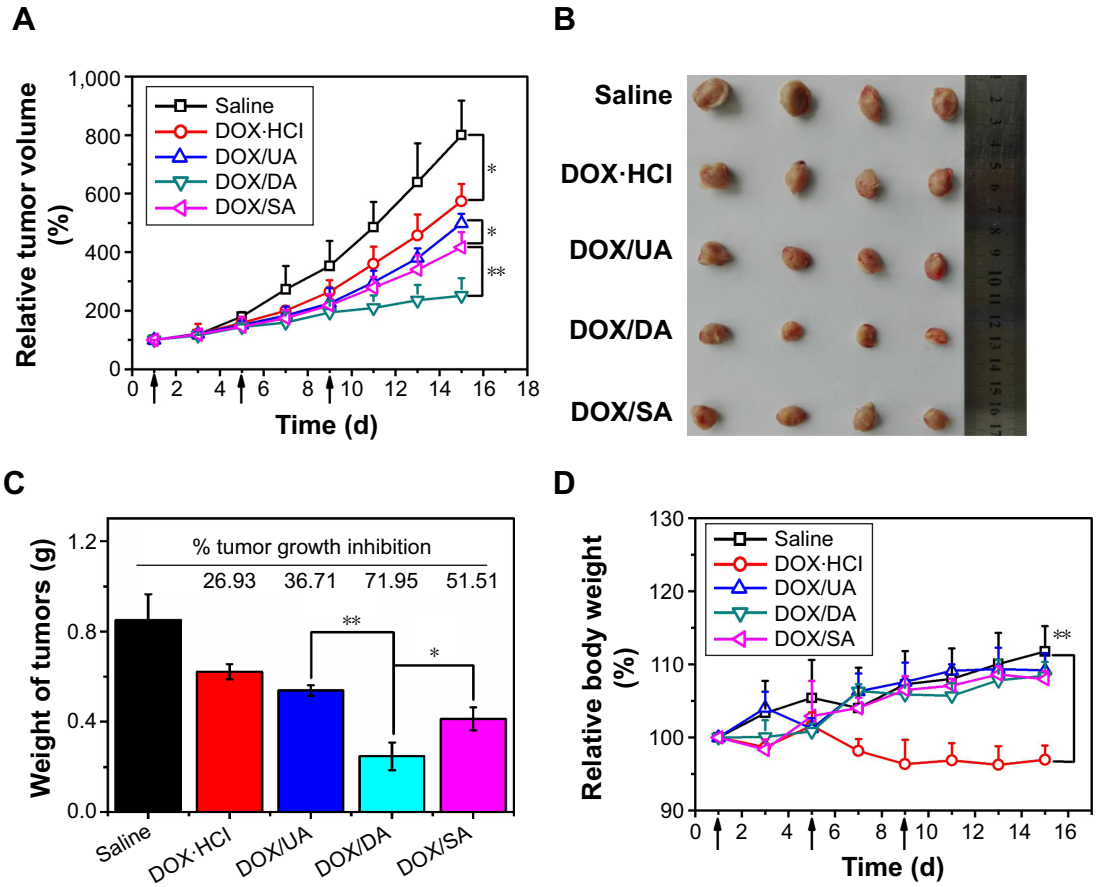

Figure 7 Antitumor effect in vivo. Relative tumor volumes of each group during the chemotherapy period, injected on days 1, 5, and 9 (**A**). Graphics of solid tumors in each group on day 15 (**B**). Tumor weight in each group after treatment (**C**). Relative body weight of mice (**D**).
Note: Statistical significance is shown as $^{**}P<0.01$, and $^{*}P<0.5$.
Abbreviations: DA, dimethylmaleic acid; DOX, doxorubicin; DOX·HCl, doxorubicin hydrochloride; SA, succinic anhydride; UA, urocanic acid.

Antitumor effects

Different formulations of DOX were injected into tumor-bearing mice to evaluate the antitumor effects and systemic toxicity. As shown in Figure 7, among the DOX-loaded NPs groups, DOX/DA exhibited the superior antitumor effect in vivo (70.9%±7.1% tumor growth inhibition), which benefited from the most remarkable targeting efficiency to tumor tissues, enhanced cellular uptake by tumor cells, and rapid intracellular release of DOX. DOX·HCl, which lacked targeting effect, exhibited unsatisfactory antiproliferation effect in vivo in spite of higher cytotoxicity against 4T1 cells in vitro and showed significant loss in weight.[40] In summary, DOX-loaded NPs, particularly DOX/DA, with an on-demand DOX release and targeting efficiency to tumor in vivo, showed enhanced therapeutic effect and reduced side effect.

Conclusion

In this study, we developed novel stepwise pH-responsive NPs for DOX delivery, which could respond to both extracellular pH and intracellular pH. With a negative zeta potential in physiological condition, DA-NPs exhibited good stability during the blood circulation, with low nonspecific adsorption to serum protein. In combination with the EPR effect, DA-NPs gained an enhanced passive targeting effect to solid tumors. Responding to the extracellular pH of tumor cells, these NPs reversed its zeta potential from negative to positive and enhanced the cellular uptake. After internalization, DOX released rapidly from DOX/DA, triggered by the endo/lysosomal pH, thereby leading to the apoptosis of tumor cells. In summary, the stepwise pH-responsive NPs exhibited an enhanced antitumor efficiency and reduced side effect in vivo.

Acknowledgments

This work was supported by the National Natural Science Foundation Projects of China (Nos 81571788 and 81273463), Jiangsu Science and Technology Support Plan (BE 2011670), and Priority Academic Program Development of Jiangsu Higher Education Institutions (PAPD). The authors thank Ms Wenjing Zhu for her contribution in data analysis.

Disclosure

The authors report no conflicts of interest in this work.

References

1. Cully M. Drug delivery: nanoparticles improve profile of molecularly targeted cancer drug. *Nat Rev Drug Discov*. 2016;15(4):231.
2. Huang Y, Wang YJ, Wang Y, et al. Exploring naturally occurring ivy nanoparticles as an alternative biomaterial. *Acta Biomater*. 2015;25: 268–283.
3. Mo R, Sun Q, Xue J, et al. Multistage pH-responsive liposomes for mitochondrial-targeted anticancer drug delivery. *Adv Mater*. 2012; 24(27):3659–3665.
4. Albanese A, Tang PS, Chan WC. The effect of nanoparticle size, shape, and surface chemistry on biological systems. *Annu Rev Biomed Eng*. 2012;14:1–16.
5. Wang Y, Yi S, Sun L, Huang Y, Zhang M. Charge-selective fractions of naturally occurring nanoparticles as bioactive nanocarriers for cancer therapy. *Acta Biomater*. 2014;10(10):4269–4284.
6. Maeda H. Macromolecular therapeutics in cancer treatment: the EPR effect and beyond. *J Control Release*. 2012;164(2):138–144.
7. Han SS, Li ZY, Zhu JY, et al. Dual-pH sensitive charge-reversal polypeptide micelles for tumor-triggered targeting uptake and nuclear drug delivery. *Small*. 2015;11(21):2543–2554.
8. Zhou T, Zhou X, Xing D. Controlled release of doxorubicin from graphene oxide based charge-reversal nanocarrier. *Biomaterials*. 2014; 35(13):4185–4194.
9. Du JZ, Mao CQ, Yuan YY, Yang XZ, Wang J. Tumor extracellular acidity-activated nanoparticles as drug delivery systems for enhanced cancer therapy. *Biotechnol Adv*. 2014;32(4):789–803.
10. Yuan YY, Mao CQ, Du XJ, Du JZ, Wang F, Wang J. Surface charge switchable nanoparticles based on zwitterionic polymer for enhanced drug delivery to tumor. *Adv Mater*. 2012;24(40):5476–5480.
11. Li F, Chen W, You B, et al. Enhanced cellular internalization and on-demand intracellular release of doxorubicin by stepwise pH-/reduction-responsive nanoparticles. *ACS Appl Mater Interfaces*. 2016; 8(47):32146–32158.
12. Li J, Yu X, Wang Y, et al. A reduction and pH dual-sensitive polymeric vector for long-circulating and tumor-targeted siRNA delivery. *Adv Mater*. 2014;26(48):8217–8224.
13. Du JB, Cheng Y, Teng ZH, et al. pH-triggered surface charge reversed nanoparticle with active targeting to enhance the antitumor activity of doxorubicin. *Mol Pharm*. 2016;13(5):1711–1722.
14. Mura S, Nicolas J, Couvreur P. Stimuli-responsive nanocarriers for drug delivery. *Nat Mater*. 2013;12(11):991–1003.
15. Li Y, Xiao K, Zhu W, Deng W, Lam KS. Stimuli-responsive cross-linked micelles for on-demand drug delivery against cancers. *Adv Drug Deliv Rev*. 2014;66:58–73.
16. Wang Y, Zhou K, Huang G, et al. A nanoparticle-based strategy for the imaging of a broad range of tumours by nonlinear amplification of microenvironment signals. *Nat Mater*. 2014;13(2):204–212.
17. Liu J, Huang Y, Kumar A, et al. pH-sensitive nano-systems for drug delivery in cancer therapy. *Biotechnol Adv*. 2014;32(4):693–710.
18. Zhou K, Wang Y, Huang X, Luby-Phelps K, Sumer BD, Gao J. Tunable, ultrasensitive pH-responsive nanoparticles targeting specific endocytic organelles in living cells. *Angew Chem Int Ed Engl*. 2011;50(27): 6109–6114.
19. Wang Y, Chen H, Liu Y, et al. pH-sensitive pullulan-based nanoparticle carrier of methotrexate and combretastatin A4 for the combination therapy against hepatocellular carcinoma. *Biomaterials*. 2013;34(29):7181–7190.
20. Li Y, Yang J, Xu B, Gao F, Wang W, Liu W. Enhanced therapeutic siRNA to tumor cells by a pH-sensitive agmatine-chitosan bioconjugate. *ACS Appl Mater Interfaces*. 2015;7(15):8114–8124.
21. Jiang L, Li L, He X, et al. Overcoming drug-resistant lung cancer by paclitaxel loaded dual-functional liposomes with mitochondria targeting and pH-response. *Biomaterials*. 2015;52:126–139.
22. Xiao B, Ma P, Viennois E, Merlin D. Urocanic acid-modified chitosan nanoparticles can confer anti-inflammatory effect by delivering CD98 siRNA to macrophages. *Colloids Surf B Biointerfaces*. 2016;143: 186–193.
23. Li L, Yang Q, Zhou Z, Zhong J, Huang Y. Doxorubicin-loaded, charge reversible, folate modified HPMA copolymer conjugates for active cancer cell targeting. *Biomaterials*. 2014;35(19):5171–5187.
24. Feng Q, Yu MZ, Wang JC, et al. Synergistic inhibition of breast cancer by co-delivery of VEGF siRNA and paclitaxel via vapreotide-modified core-shell nanoparticles. *Biomaterials*. 2014;35(18):5028–5038.
25. Cui C, Xue YN, Wu M, et al. Cellular uptake, intracellular trafficking, and antitumor efficacy of doxorubicin-loaded reduction-sensitive micelles. *Biomaterials*. 2013;34(15):3858–3869.
26. Zhu QL, Zhou Y, Guan M, et al. Low-density lipoprotein-coupled N-succinyl chitosan nanoparticles co-delivering siRNA and doxorubicin for hepatocyte-targeted therapy. *Biomaterials*. 2014;35(22): 5965–5976.
27. Han HS, Choi KY, Ko H, et al. Bioreducible core-crosslinked hyaluronic acid micelle for targeted cancer therapy. *J Control Release*. 2015;200:158–166.
28. Chen W, Achazi K, Schade B, Haag R. Charge-conversional and reduction-sensitive poly(vinyl alcohol) nanogels for enhanced cell uptake and efficient intracellular doxorubicin release. *J Control Release*. 2015;205:15–24.
29. Kang B, Li J, Chang S, et al. Subcellular tracking of drug release from carbon nanotube vehicles in living cells. *Small*. 2012;8(5):777–782.
30. Yuan ZQ, Li JZ, Liu Y, et al. Systemic delivery of micelles loading with paclitaxel using N-succinyl-palmitoyl-chitosan decorated with cRGDyK peptide to inhibit non-small-cell lung cancer. *Int J Pharm*. 2015; 492(1–2):141–151.
31. Zhu A, Miao K, Deng Y, et al. Dually pH/reduction-responsive vesicles for ultrahigh-contrast fluorescence imaging and thermo-chemotherapy-synergized tumor ablation. *ACS Nano*. 2015;9(8):7874–7885.
32. Guo X, Wei X, Jing Y, Zhou S. Size changeable nanocarriers with nuclear targeting for effectively overcoming multidrug resistance in cancer therapy. *Adv Mater*. 2015;27(41):6450–6456.
33. Du JZ, Sun TM, Song WJ, Wu J, Wang J. A tumor-acidity-activated charge-conversional nanogel as an intelligent vehicle for promoted tumoral-cell uptake and drug delivery. *Angew Chem Int Ed Engl*. 2010; 49(21):3621–3626.
34. Li Z, Qiu L, Chen Q, et al. pH-sensitive nanoparticles of poly(L-histidine)-poly(lactide-co-glycolide)-tocopheryl polyethylene glycol succinate for anti-tumor drug delivery. *Acta Biomater*. 2015;11: 137–150.
35. Guan X, Li Y, Jiao Z, et al. A pH-sensitive charge-conversion system for doxorubicin delivery. *Acta Biomater*. 2013;9(8):7672–7678.
36. Qiu L, Hu Q, Cheng L, et al. cRGDyK modified pH responsive nanoparticles for specific intracellular delivery of doxorubicin. *Acta Biomater*. 2016;30:285–298.
37. Han X, Li Z, Sun J, et al. Stealth CD44-targeted hyaluronic acid supramolecular nanoassemblies for doxorubicin delivery: probing the effect of uncovalent pegylation degree on cellular uptake and blood long circulation. *J Control Release*. 2015;197:29–40.
38. Wang K, Zhang X, Liu Y, Liu C, Jiang B, Jiang Y. Tumor penetrability and anti-angiogenesis using iRGD-mediated delivery of doxorubicin-polymer conjugates. *Biomaterials*. 2014;35(30):8735–8747.
39. Bai F, Wang C, Lu Q, et al. Nanoparticle-mediated drug delivery to tumor neovasculature to combat P-gp expressing multidrug resistant cancer. *Biomaterials*. 2013;34(26):6163–6174.
40. Wang J, Xu W, Guo H, et al. Selective intracellular drug delivery from pH-responsive polyion complex micelle for enhanced malignancy suppression in vivo. *Colloids Surf B Biointerfaces*. 2015;135:283–290.

Supplementary materials

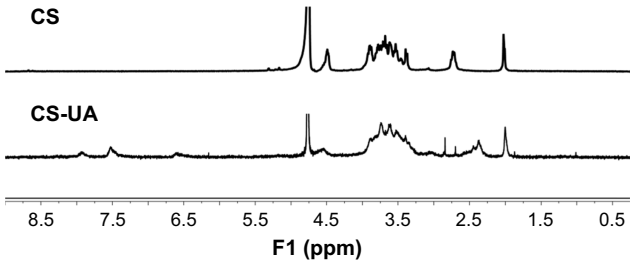

Figure S1 ^{1}H NMR spectra of CS and CS-UA. CS-UA was synthesized by reacting CS and UA. δ 7.4 refers to the hydrogen atom in imidazole group, suggesting that UA was grafted into CS.
Abbreviations: UA, urocanic acid; CS, chitosan; ^{1}H NMR, hydrogen-1 nuclear magnetic resonance; ppm, parts per million.

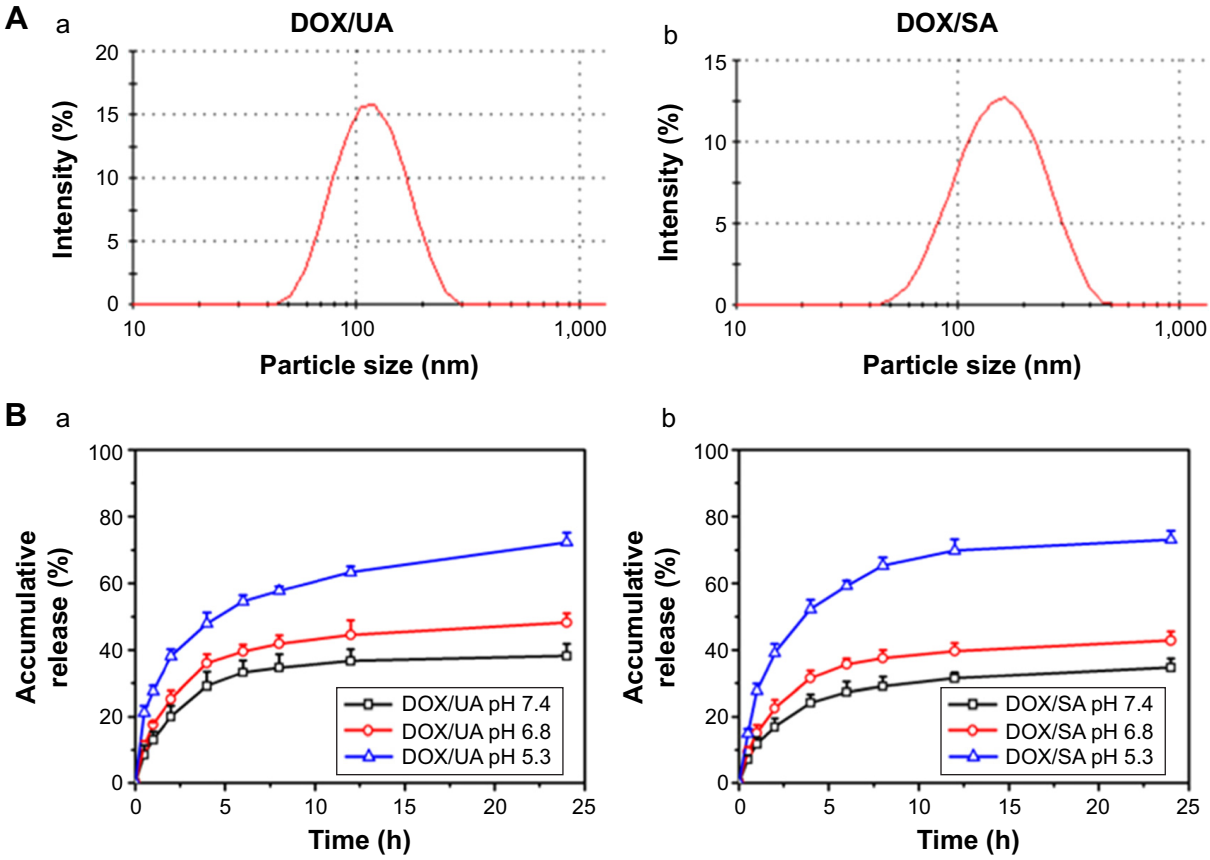

Figure S2 Particle size distribution (**A**) and DOX release (**B**) from DOX/UA and DOX/SA. DOX/UA and DOX/SA were prepared with particle size of 120–140 nm and narrow size distribution. DOX release behavior of DOX/UA and DOX/SA was similar to that of DOX/DA. DOX/UA and DOX/SA exhibited delayed DOX release at pH 7.3 and rapid DOX release at pH 5.3. The extracellular pH (pH 6.8) did not have a significant effect on the release behavior of DOX-loaded NPs.
Abbreviations: DA, dimethylmaleic acid; DOX, doxorubicin; NPs, nanoparticles; SA, succinic anhydride; UA, urocanic acid.

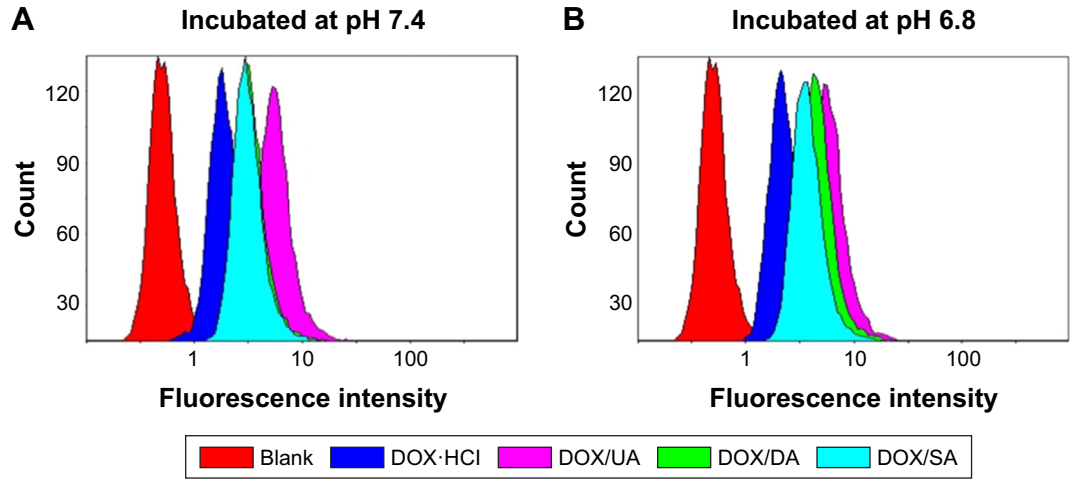

Figure S3 Quantitative uptake of DOX under different pH values using flow cytometry. Mean fluorescence intensity of 4T1 cells treated with DOX formulations. DOX-loaded NPs exhibited a higher uptake than DOX·HCl at pH 7.4 (**A**) or 6.8 (**B**). Positively charged DOX/UA had a higher uptake than negatively charged DOX/DA and DOX/SA at pH 7.4. As pH decreased from 7.4 to 6.8, the uptake of DOX/DA was significantly increased. However, decreased pH did not significantly affect the uptake of DOX·HCl DOX/UA or DOX/SA.

Abbreviations: DA, dimethylmaleic acid; DOX, doxorubicin; DOX·HCl, doxorubicin hydrochloride; NPs, nanoparticles; SA, succinic anhydride; UA, urocanic acid.

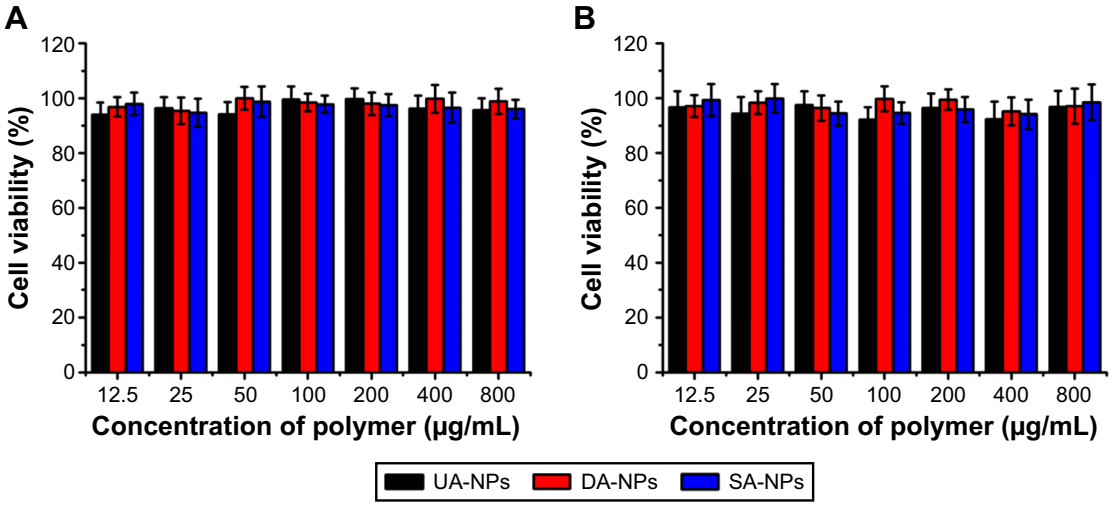

Figure S4 Cytotoxicity of blank NPs against 4T1 cells at pH 7.4 (**A**) and 6.8 (**B**). The cytotoxicity of blank NPs was evaluated via MTT assay, after incubation with 4T1 cells for 24 h. As shown in the figure, when the concentration of polymers ranged from 12.5 to 800 μg/mL, UA-NPs, DA-NPs, or SA-NPs almost had no cytotoxicity against 4T1 cells.

Abbreviations: DA, dimethylmaleic acid; DOX, doxorubicin; NPs, nanoparticles; SA, succinic anhydride; UA, urocanic acid.

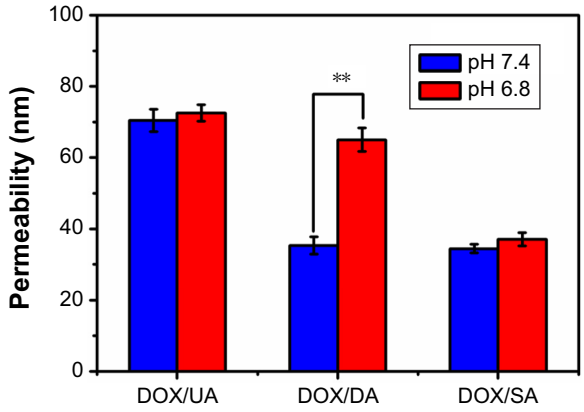

Figure S5 Permeability of DOX-NPs into 3D tumor spheres; quantitative data calculated from Figure 5.

Note: Statistical significance is shown as $^{**}P<0.01$.

Abbreviation: 3D, three dimensional; DA, dimethylmaleic acid; DOX, doxorubicin; NPs, nanoparticles; SA, succinic anhydride; UA, urocanic acid.